

The Massive Progenitor of the Type II-Linear SN 2009kr¹

Nancy Elias-Rosa², Schuyler D. Van Dyk², Weidong Li³, Adam A. Miller³, Mohan Ganeshalingam³, Andrew F. Boden⁴, Shrinivas R. Kulkarni⁴, József Vinkó^{5,6}, Jean-Charles Cuillandre⁷, Thea N. Steele³, Ryan J. Foley^{8,9}, Joshua S. Bloom³, and Alexei V. Filippenko³

ABSTRACT

We present early-time photometric and spectroscopic observations of supernova (SN) 2009kr in NGC 1832. We find that its properties to date support its classification as Type II-Linear (SN II-L), a relatively rare subclass of core-collapse supernovae (SNe). We have also identified a candidate for the SN progenitor star through comparison of pre-explosion, archival images obtained using WFPC2 onboard the *Hubble Space Telescope* (*HST*) with SN images obtained using adaptive optics (AO) plus NIRC2 on the 10-m Keck II telescope. Although the host galaxy's distance (~ 26 Mpc) results in large uncertainties in the relative astrometry, if this candidate is indeed the progenitor, it is a highly luminous ($M_V^0 = -7.8$ mag) yellow supergiant with initial mass $\sim 18\text{--}24 M_\odot$. This would be the first time that a SN II-L progenitor has been directly identified. Its mass may be a bridge between the upper initial mass limit for the more common Type II-Plateau SNe (SNe II-P) and the inferred initial mass estimate for one Type II-narrow SN (SN IIn).

Subject headings: galaxies: individual (NGC 1832) — stars: evolution — supernovae: general — supernovae: individual (SN 2009kr)

²Spitzer Science Center, California Institute of Technology, 1200 E. California Blvd., Pasadena, CA 91125; email nelias@ipac.caltech.edu.

³Department of Astronomy, University of California, Berkeley, CA 94720-3411.

⁴Division of Physics, Math, and Astronomy, California Institute of Technology, Pasadena, CA 91125.

⁵Department of Optics & Quantum Electronics, University of Szeged, Dóm tér 9, Szeged H-6720, Hungary.

⁶Department of Astronomy, University of Texas, Austin, TX 78712.

⁷Canada-France-Hawaii Telescope Corporation, 65-1238 Mamalahoa Hwy, Kamuela, HI 96743.

⁸Harvard-Smithsonian Center for Astrophysics, 60 Garden Street, Cambridge, MA 02138.

⁹Clay Fellow.

1. Introduction

It is not yet exactly clear how to map massive stars of a given mass range to a core-collapse supernova (CC-SN) type. We now know with a growing degree of confidence that solitary stars in the range of $\sim 8\text{--}16\ M_\odot$ inevitably explode as the SNe II-P (e.g., Li et al. 2007; Smartt et al. 2009), with much of their hydrogen envelopes still intact. We also have evidence that the SN IIn 2005gl had a luminous ($M_V = -10.3$ mag), very massive (possibly with $M_{\text{ini}} > 50\ M_\odot$) progenitor star that exploded while in the luminous blue variable phase (Gal-Yam & Leonard 2009). This progenitor, the only example so far identified for a SN IIn, likely had a far smaller fraction of its outer H layer remaining than SNe II-P. Various indirect clues may indicate that at least some of the Type Ib/c SNe are connected to the Wolf-Rayet phase, which is expected to occur for stars with $M_{\text{ini}} > 25\text{--}30\ M_\odot$ (e.g., Crowther 2007). That leaves the Type II-L SNe with no directly known progenitor star, as well as the initial mass range $18 \lesssim M_{\text{ini}}(M_\odot) \lesssim 30$ (exactly the range that Smartt et al. 2009 dubbed “the red supergiant problem”) without a well-established endpoint. From the SN rates derived from the Lick Observatory Supernova Search (Li et al. 2010, in prep.), we know that the majority of massive stars end their lives as SNe II-P, while the incidences of SNe II-L and SNe IIn are comparatively rare ($\sim 7\%$ and $\sim 6\%$ of all CC-SNe, respectively).

Here we examine the case of SN 2009kr in NGC 1832. SN 2009kr was discovered by Nakano & Itagaki (2009) on 2009 November 6.73 (UT dates are used throughout) and was spectroscopically classified as a SN IIn (Tendulkar et al. 2009), and then as a “young type-II” SN (Steele et al. 2009). Li et al. (2009b) first identified a possible progenitor star in high spatial resolution archival *HST* images from 2004, using as reference a combined 160-s r' image from the 3.6-m Canada-France-Hawaii Telescope (CFHT)+MegaCam on November 21.49. Here we show that both early-time photometric and spectroscopic observations strongly suggest that this object is a SN II-L, and we increase our confidence in the progenitor identification via further comparison of the *HST* images with Keck II/NIRC2 + adaptive optics (AO) data.

¹Based in part on observations made with the NASA/ESA *Hubble Space Telescope*, obtained from the Data Archive at the Space Telescope Science Institute, which is operated by the Association of Universities for Research in Astronomy (AURA), Inc., under NASA contract NAS 05-26555; and on observations obtained at the W. M. Keck Observatory, which is operated as a scientific partnership among the California Institute of Technology, the University of California, and NASA; the observatory was made possible by the generous financial support of the W. M. Keck Foundation.

2. The Early-Time Nature of SN 2009kr

2.1. Photometry

Optical *BVRI* images of SN 2009kr were obtained with the 0.76-m Katzman Automatic Imaging Telescope (KAIT; Filippenko et al. 2001) and the 1.0-m Nickel Telescope at Lick Observatory. They were all initially reduced using standard procedures. Because of our follow-up campaign on SN 2004gq, also in NGC 1832 (Modjaz 2007), we had a well-calibrated photometric sequence in the host-galaxy field and template images in all passbands for image subtraction. We used a photometry reduction pipeline (Ganeshalingam et al. 2010) to reduce all data and calibrate the photometry to the standard Johnson *BV* and Cousins *RI* system.

Near-infrared (NIR) observations were obtained with the 1.3-m Peters Automated Infrared Imaging Telescope (PAIRITEL; Bloom et al. 2006) and reduced using standard procedures. We used archival 2MASS (Skrutskie et al. 2006) images of NGC 1832 as templates to subtract from the SN images using HOTPANTS¹⁰ and calibrated the *JHK_s* photometry against 2MASS stars in the field.

The *BVRIJHK_s* light curves are shown in Figure 1 [panel (a)], relative to *B*-band maximum (15.95 ± 0.02 mag on Nov 13 ± 1 , or JD 2455149 ± 1). For comparison, we also show the light curves of the SN II-L 1980K (Buta 1982; Dwek et al. 1983); the SN II-P 1999em (Hamuy et al. 2001; Leonard et al. 2002; Elmhamdi et al. 2003); and, the possible SN II-L 2000dc (Poznanski et al. 2009), with which we find the best match. The SN 2009kr light curves can also be well matched to two other published SNe II-L, not shown: SN 1979C (Balinskaia et al. 1980; de Vaucouleurs et al. 1981; Barbon et al. 1982) and SN 1990K (Cappellaro et al. 1995). SN 2009kr does not follow the SN II-P plateau; instead, it more closely resembles the SN II-L linear decline (see Barbon, Ciatti, & Rosino 1979).

We also find that the SN 2009kr colors agree well with the SNe II-L. Although a “standard” color evolution for SNe II-L has not yet been established, and it is possible that they are heterogeneous, our color comparison implies low reddening toward SN 2009kr, consistent with what is found from its spectra (see § 2.2).

From our adopted distance and total extinction (see §2.2), SN 2009kr reached $M(B_{\max}) = -16.48 \pm 0.30$ mag, typical of SNe II-L (Young & Branch 1989). The $M(R_{\max}) = -17.06 \pm 0.30$ mag is also within the scatter around the average of a SN II-L sample studied by Li et al. (2010, in prep.). We thus conclude that SN 2009kr displays the photometric behavior of

¹⁰<http://www.astro.washington.edu/users/becker/hotpants.html>.

a SN II-L.

2.2. Spectroscopy

Low-resolution spectra of SN 2009kr were obtained on November 10 and 25, and December 9, with the Kast spectrograph on the Lick 3-m Shane telescope (Miller & Stone 1993). The spectra were reduced and calibrated using standard procedures (e.g., Matheson et al. 2000). The observing conditions were not photometric during any of the nights, resulting in an uncertain absolute flux calibration. We observed with the slit placed at the parallactic angle (Filippenko 1982).

We show the rest-frame spectral sequence in Figure 1, panel (b); for comparison, we also provide spectra of the SN II-P 1999em (Leonard et al. 2002) and the SN II 2001cy (data previously unpublished) at similar epochs. Poznanski et al. (2009) rejected SN 2001cy from their SN II-P sample, implying that it may likely be a SN II-L. Indeed, the SN 2001cy light curve is very similar (but of inferior quality and coverage) to that of SN 2000dc shown in panel (a). SN 1999em has been corrected for a $E(B - V)_{tot} = 0.10$ mag (Leonard et al. 2002), SN 2009kr for $E(B - V) = 0.08$ mag (see below), and SN 2001cy has been corrected only for Galactic reddening, $E(B - V) = 0.206$ mag (Schlegel, Finkbeiner, & Davis 1998).

The spectral sequence for SN 2009kr is typical of many SNe II: the earliest spectrum exhibits a blue continuum, with relatively weak spectral features, followed by the onset of increased Balmer-line emission, together with the emergence of P-Cygni-like features. However, clearly it differs from the canonical SN II-P 1999em; in particular, the SN 2009kr P-Cygni $H\alpha$ profile is dominated by the emission component. Several narrow emission lines appear superposed on the spectra, but these most likely originate from a neighboring H II region. The SN 2009kr spectra more closely resemble those of the SN II 2001cy, which also exhibits relatively weak $H\alpha$ absorption. The optical photometric declines [$\gtrsim 1$ mag (100 day) $^{-1}$] of both SNe 2001cy and 2009kr suggest that they are SNe II-L (see § 2.1). Since spectroscopic features of SNe II appear to be correlated with their photometric behavior at early times (Schlegel 1996; Filippenko 1997), the similarities in the SNe 2001cy and 2009kr spectra are not unexpected.

We also obtained a high-resolution optical spectrum of the SN on November 25.46 with the CHFT + echelle spectropolarimetric ESPaDOnS, with 4 exposures of 833 s each, from which we confirm that the narrow $H\alpha$ emission originates from a H II region. Moreover, we also used this spectrum to estimate the reddening toward SN 2009kr via measurement of the Na I D equivalent width (EW) at the host-galaxy redshift ($z = 0.006$). We found $EW(\lambda 5890)$

$= 0.044 \pm 0.003 \text{ \AA}$ and $\text{EW}(\lambda 5896) = 0.032 \pm 0.004 \text{ \AA}$ for the D1 and D2 components, respectively. Using the relation between extinction and $\text{EW}(\text{Na I D})$ from Elias-Rosa et al. (2010, in prep.), and assuming the Cardelli, Clayton, & Mathis (1989) reddening law with updated wavelengths and a Galactic foreground $E(B - V) = 0.07 \text{ mag}$ (Schlegel et al. 1998), we derive $E(B - V)_{\text{tot}} = 0.08 \pm 0.01 \text{ mag}$ ($E[V - I]_{\text{tot}} = 0.11 \pm 0.01 \text{ mag}$). This relatively low extinction is consistent with both the SN color comparison (§ 2.1) and the overall blue continua seen in the early SN 2009kr spectra (Figure 1, panel [b]). We therefore adopt this value for SN 2009kr.

3. Identification of the Progenitor Candidate

Pairs of *HST* images of NGC 1832 were obtained with WFPC2 in bands F555W ($\sim V$; 460 s total) and F814W ($\sim I$; 700 s total) on 2008 January 11 (program GO-10877, PI: W. Li), as SN 2004gq follow-up observations. The SN 2009kr site is located on the WF3 chip ($0''.1 \text{ pixel}^{-1}$). Cosmic-ray hits were rejected, and a $1600 \times 1600 \text{ pixel}^2$ mosaic of all four WFPC2 chips was constructed using the STSDAS package routines *crrej* and *wmosaic* within IRAF¹¹. Li et al. (2009b) were able to isolate the SN location in the WFPC2 images to 0.43 pixel ($0''.043$) through comparison with a ground-based, post-explosion CFHT/MegaCam image.

We were then able to better confirm the identification of this candidate through K_p -band NIRC2 “wide” camera ($0''.04 \text{ pixel}^{-1}$, field-of-view $40'' \times 40''$) images obtained on November 28 with the Keck II 10-m Telescope+AO. Each of the 10 s frames was sky subtracted using the median of the dithered exposures, and then “shifted-and-added” using IRAF. They were also corrected for distortion¹².

We achieved high-precision relative astrometry by geometrically transforming the pre-explosion images to match the post-explosion ones. We first “drizzled”¹³ the pre-explosion images for each band to the higher NIRC2+AO resolution. Using 5–7 point-like sources in common between the two datasets and the IRAF task *geomap*, we carried out a geometrical transformation between the two sets of coordinates. The positions (and their uncertainties)

¹¹IRAF (Image Reduction and Analysis Facility) is distributed by the National Optical Astronomy Observatories, which are operated by the AURA, Inc., under cooperative agreement with the National Science Foundation.

¹²http://www2.keck.hawaii.edu/inst/nirc2/forReDoc/post_observing/dewarp/

¹³<http://www.stsci.edu/hst/wfpc2/analysis/drizzle.html>.

for the SN and the progenitor candidate are derived by averaging the measurements from two centroiding methods, the task *daofind* within IRAF/DAOPHOT and *imexamine* within IRAF. Note that no other source was located within a 3σ radius from the progenitor candidate position identified by Li et al. (2009b) (see Figure 2). The differences between the SN and the progenitor candidate positions, compared with the total estimated astrometric uncertainty are given in Table 1. As an additional check, we transformed the NIRC2+AO image relative to only the WF3 chip image in F814W at its native resolution ($0''.1 \text{ pixel}^{-1}$) and performed the registration. In this case, the positional difference is 19 mas, within $\sim 1\sigma$ of the astrometric solution.

4. The Nature of the Progenitor

We also measured photometry of these *HST* images using HSTphot¹⁴ (Dolphin 2000). The output from this package automatically includes the transformation from F555W and F814W to V and I .

Adopting a distance modulus to NGC 1832 derived from the recession velocity corrected for the Virgo infall (32.09 ± 0.30 mag, where the uncertainty arises from a possible 250 km s^{-1} peculiar velocity; NED¹⁵) and the assumed SN extinction, we find that the absolute magnitudes of the progenitor candidate are $M_V^0 = -7.80 \pm 0.33$ and $M_I^0 = -8.75 \pm 0.32$, entirely consistent with a highly luminous supergiant. The intrinsic color, $(V - I)_0 = 0.95 \pm 0.46$ mag, is significantly more “yellow” than the colors of normal red supergiants (RSGs).

We can directly determine the metallicity in the SN environment from the CFHT high-resolution spectrum, by measuring the $H\alpha$ and $[\text{N II}] \lambda 6584 \text{ \AA}$ line intensities and applying the cubic-fit relation between the ratio of these two lines and the oxygen abundance, from Pettini & Pagel (2004); no correction is made for the low extinction. Doing so, we find that $12 + \log(\text{O}/\text{H}) = 8.67$. Given that the solar $12 + \log(\text{O}/\text{H}) = 8.69 \pm 0.05$ (Asplund, Grevesse, Sauval & Scott 2009), we consider it most likely that this environment has solar metallicity.

The star’s color corresponds to a bolometric correction -0.26 mag and an effective temperature $T_{\text{eff}} \approx 5300 \pm 250 \text{ K}$ (this uncertainty is based on the uncertainty in the bolometric

¹⁴HSTphot is a stellar photometry package designed for use with *HST* WFPC2 images. We used v1.1.7b, updated 2008 July 19.

¹⁵<http://nedwww.ipac.caltech.edu/>.

correction estimation), for an assumed surface gravity $\log g = +0.5$ (according to the Kurucz Atlas 9 models, Kurucz 1993). This results in $L_{\text{bol}} = 10^{(5.12 \pm 0.13)} L_{\odot}$ (assuming $M_{\text{bol}}(\odot) = 4.74$). In Figure 3 we show a Hertzsprung-Russell (HR) diagram, including the progenitor candidate. In addition, we also show model evolutionary tracks (Hirschi, Meynet, & Maeder 2004) for stars with initial masses $M_{\text{ini}} = 15, 20$, and $25 M_{\odot}$, with rotation ($v_{\text{ini}} = 300 \text{ km s}^{-1}$) and without rotation.

The location of the progenitor candidate in the HR diagram is clearly not consistent with the $15 M_{\odot}$ tracks, an initial mass which lies within the range for SN II-P progenitors (Smartt et al. 2009). Unfortunately, the mass bins for these tracks are large (in “quanta” of $5 M_{\odot}$). However, taking into account the uncertainty in the progenitor candidate’s luminosity, interpolating by eye between the tracks implies that $M_{\text{ini}} \simeq 18\text{--}24 M_{\odot}$. We note that this is consistent with the upper limit placed on the SN 1980K progenitor (Thompson 1982), $< 20 M_{\odot}$, using more current theoretical tracks (Smartt et al. 2009), and the lower limit, $17\text{--}18 M_{\odot}$, for the SN II-L 1979C progenitor (Van Dyk et al. 1999).

That such a massive progenitor would be somewhat bluer than would be expected for the normal RSG progenitors of SNe II-P is also consistent with the star being in a post-RSG phase. Such an expectation follows from the theoretical models by Hirschi et al. (2004) for rotating stars at higher masses. As Hirschi et al. note, the rotating models are more luminous and evolve to the RSG phase before the ignition of He burning, which results in higher mass-loss rates, the loss of most of the H envelope before the termination of He burning, and evolution toward the blue before the terminal points. From Figure 3 one can see that rotation makes little difference in the evolution of a $15 M_{\odot}$ star; both the rotating and non-rotating tracks terminate as a RSG. However, for a $20 M_{\odot}$ star, rotation has a profound evolutionary effect. Though we cannot tell from these models what occurs for stars in the $15\text{--}20 M_{\odot}$ range, it is reasonable to assume that rotation begins to affect those models nearing $20 M_{\odot}$. Thus, we might expect the progenitor candidate, based on our mass estimate above, to have evolved toward the blue before explosion.

Although more luminous and hotter than the SN 2009kr progenitor candidate, similar behavior has been found for the post-RSG star IRC+10420, a mass-losing hypergiant that is transiting the so-called “yellow void” (Humphreys et al. 2002). Likely more analogous are the “anomalous” yellow supergiants in the Magellanic Clouds, which are in the mass range $15\text{--}20 M_{\odot}$ and show evidence for post-RSG evolution (Humphreys et al. 1991). We note that these stars are at subsolar metallicity.

Of course, there are caveats to our discussion above. As we found for the peculiar SN II-P 2008cn (Elias-Rosa et al. 2009), a yellow progenitor color could result from evolution in an interacting binary. Additionally, although the difference between the SN and progenitor

candidate positions are practically within the total uncertainties, these are still large, and, given the host galaxy’s distance (a single NIRC2 pixel corresponds to ~ 5 pc), the possibility still distinctly exists that we have not identified the SN progenitor at all, but rather a compact star cluster. If so, adopting the SN extinction, we can fit the V and I fluxes for the candidate with the Starburst99 code¹⁶ model spectral energy distributions and find an excellent fit with a 10 Myr track (Figure 4). If the SN progenitor were a member of this cluster, this age estimate would still be consistent with the lifespan of a $\sim 20 M_{\odot}$ star. We note, however, that if this is a cluster, it would be of very low luminosity; we would ordinarily expect compact star clusters to have $M_V < -8.6$ mag (Bastian et al. 2005; Crockett et al. 2008). Further dust obscuration, beyond our assumed extinction, would imply that the putative cluster could be more luminous, but also bluer and younger. If the SN 2009kr progenitor is not associated with the candidate and has not been detected in the pre-SN *HST* images, then by inserting artificial stars near the SN site using HSTphot, we find $L_{\text{bol}} \lesssim 10^{(4.7 \pm 0.1)} L_{\odot}$ and $M_{\text{ini}} \lesssim 14 M_{\odot}$ for an undetected progenitor.

A similar study has been done contemporaneously by Fraser et al. (2009). Both studies identify the same candidate progenitor. However, Fraser et al. (2009) suggest that the SN is a spectrally peculiar SN II-P, with only r -band photometry reported. Differences also exist in the metallicity estimate and theoretical models employed, leading to somewhat different estimates for M_{ini} ($15^{+5}_{-4} M_{\odot}$ in Fraser et al. 2009).

5. Conclusions

We have demonstrated, based on ~ 1 month of follow-up from discovery, that SN 2009kr is a SN II-L, a relatively rare subclass of CC-SNe. We have identified an object in pre-explosion *HST* images which agrees astrometrically with the SN 2009kr position, using NIR SN images obtained with NIRC2+AO on Keck. From the SN distance and extinction we find that the object is consistent with a highly luminous supergiant star. Placing the inferred L_{bol} and T_{eff} of the progenitor candidate on an HR diagram, we can infer $M_{\text{ini}} \sim 18\text{--}24 M_{\odot}$. Its yellow color implies that the star may have exploded in a post-RSG evolutionary state, which is predicted by our assumed theoretical stellar models. If this star is the SN 2009kr progenitor, this would be *the first-ever direct identification of a SN II-L progenitor*. The star’s mass estimate also may be a link between the upper mass range for SNe II-P (Smartt et al. 2009) and the estimated progenitor mass for one SN IIn, SN 2005gl (Gal-Yam & Leonard 2009).

¹⁶<http://www.stsci.edu/science/starburst99/>, Vazquez & Leitherer (2005).

We will continue to monitor the photometric and spectroscopic evolution of SN 2009kr, and we will also attempt to further improve the astrometric precision for the SN. Ultimately, the definitive indication that we have identified the SN progenitor is through very late-time imaging, e.g. with *HST* (Maund & Smartt 2009). However, as a SN II-L, akin to the long-lasting SN 1979C (Milisavljevic et al. 2009), we may have to wait at least a decade to image the SN site using the *James Webb Space Telescope*.

We thank C. Blake, E. Falco, M. Modjaz, J. Silverman, and D. Starr for their assistance. J.V. received support from Hungarian OTKA Grant K76816, NSF Grant AST-0707769, and Texas Advanced Research Project grant ARP-0094. A.V.F.’s group and KAIT are supported by NSF grant AST-0908886, the Sylvia & Jim Katzman Foundation, the TABASGO Foundation, and NASA through grants AR-11248 and GO-10877 from STScI. PAIRITEL is operated by SAO with support from the Harvard University Milton Fund, UC Berkeley, University of Virginia, and NASA/Swift grant NNX09AQ66G. J.S.B. and his group are partially funded by a DOE SciDAC grant.

Facilities: HST (WFPC2), Lick: KAIT, Nickel, CFHT:MegaCam, Keck-II: NIRC2+AO

REFERENCES

- Asplund, M., Grevesse, N., Sauval, A. J. & Scott, P. 2009, *A&A Rev.*, 47, 481
- Balinskaia, I. S., Bychkov, K. V., & Neizvestnyi, S. I. 1980, *A&A*, 85, L19
- Barbon, R., Ciatti, F., & Rosino, L. 1979, *A&A*, 72, 287
- Barbon, R., Ciatti, F., Rosino, L., Ortolani, S., & Rafanelli, P. 1982, *A&A*, 116, 43
- Bastian, N., Gieles, M., Efremov, Y. N., & Lamers, H. J. G. L. M. 2005, *A&A*, 443, 79
- Bloom, J. S. et al. 2006, in *Astronomical Data Analysis Software and Systems XV*, ed. C. Gabriel, et al. (San Francisco: ASP, vol. 331), 751
- Buta, R. J. 1982, *PASP*, 94, 578
- Cappellaro, E., Danziger, I. J., Della Valle, M., Gouiffes, C., & Turatto, M. 1995, *A&A*, 293, 723
- Cardelli, J. A., Clayton, G. C., & Mathis, J. S. 1989, *ApJ*, 345, 245
- Crockett, R. M., et al. 2008, *ApJ*, 672, L99

- Crowther, P. A. 2007, *ARA&A*, 45, 177
- de Vaucouleurs, G., de Vaucouleurs, A., Buta, R., Ables, H. D., & Hewitt, A. V. 1981, *PASP*, 93, 36
- Dolphin, A. E. 2000, *PASP*, 112, 1383
- Dwek, E., et al. 1983, *ApJ*, 274, 168
- Elias-Rosa, N., et al. 2009, *ApJ*, 706, 1174
- Elias-Rosa, N., et al. 2010, in prep.
- Elmhamdi, A., et al. 2003, *MNRAS*, 338, 939
- Filippenko, A. V. 1982, *PASP*, 94, 715
- Filippenko, A. V. 1997, *ARA&A*, 35, 309
- Filippenko, A. V., Li, W., Treffers, R. R., & Modjaz, M. 2001, in *Small Telescope Astronomy on Global Scales*, ed. W. P. Chen, C. Lemme, & B. Paczyński (San Francisco: ASP), 121
- Fraser, M., et al. 2009, *ApJL*, submitted (arXiv: 0912.2071)
- Gal-Yam, A., & Leonard, D. C. 2009, *Nature*, 458, 865
- Ganeshalingam, M., et al. 2010, *ApJSS*, submitted
- Hamuy, M., et al. 2001, *ApJ*, 558, 615
- Hirschi, R., Meynet G., & Maeder A. 2004, *A&A*, 425, 649
- Humphreys, R. M., Davidson, K., & Smith, N. 2002, *AJ*, 124, 1026
- Humphreys, R. M., Kudritzki, R. P., & Groth, H. G. 1991, *A&A*, 245, 593
- Kurucz, R. L., 1993, *CDROM* 13, 18
- Leonard, D. C., et al. 2002, *PASP*, 114, 35
- Li, W., et al. 2007, *ApJ*, 661, 1013
- Li, W., et al. 2009b, *Central Bureau Electronic Telegrams* 2042, 1
- Matheson T., Filippenko A. V., Ho L. C., Barth A. J., Leonard D. C., 2000, *AJ*, 120, 1499

- Maund, J. R., & Smartt, S. J. 2009, *Science*, 324, 486
- Milisavljevic, D., Fesen, R. A., Kirshner, R. P., & Challis, P. 2009, *ApJ*, 692, 839
- Miller, J. S., & Stone, R. P. S., 1993, Lick Observatory Technical Report No. 66, University of California, Santa Cruz
- Modjaz, M. 2007, Ph.D. Thesis, Harvard University
- Nakano, S., & Itagaki, K. 2009, Central Bureau Electronic Telegrams 2006, 1
- Pettini, M. & Pagel, B. E. J. 2004, *MNRAS*, 348, 59
- Poznanski D., et al., 2009, *ApJ*, 694, 1067
- Schlegel, E. M. 1996, *AJ*, 111, 1660
- Schlegel, D. J., Finkbeiner, D. P., & Davis, M. 1998, *ApJ*, 500, 525
- Skrutskie, M. F., et al. 2006, *AJ*, 131, 1163
- Smartt, S. J., et al. 2009, *MNRAS*, 395, 1409
- Steele, T. N. et al. 2009, Central Bureau Electronic Telegrams 2011, 1
- Tendulkar, S. P., et al. 2009, The Astronomer’s Telegram 2291, 1
- Thompson, L. A. 1982, *ApJ*, 257, L63
- Van Dyk, S. D., et al. 1999, *PASP*, 111, 313
- Vazquez, G. A., & Leitherer, C. 2005, *ApJ*, 621, 695
- Young, T. R., & Branch, D. 1989, *ApJ*, 342, L79

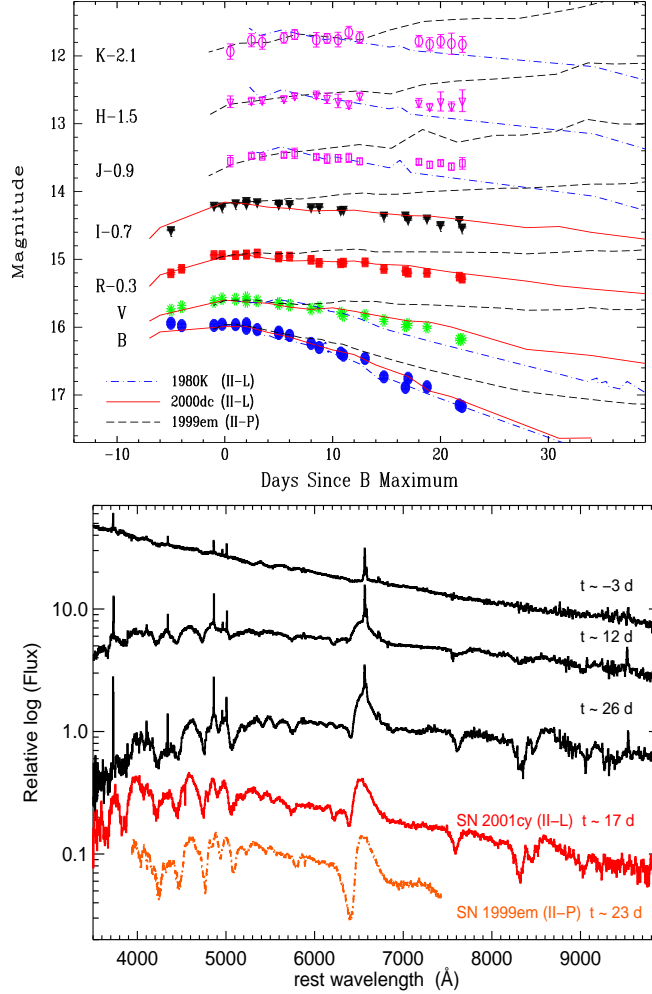


Fig. 1.— (a) SN 2009kr optical and NIR light curves, together with those of SN II-L 1980K (*dot-dashed lines*, SN II-P 1999em (*dashed lines*, and SN 2000dc (*solid lines*. (b) SN 2009kr spectral sequence, along with comparison spectra of SN II 2001cy (red line) and SN II-P 1999em (*dot-dashed*, orange line); all have been corrected for their host-galaxy recession velocities and for reddening (see text). Ages are relative to *B* maximum light.

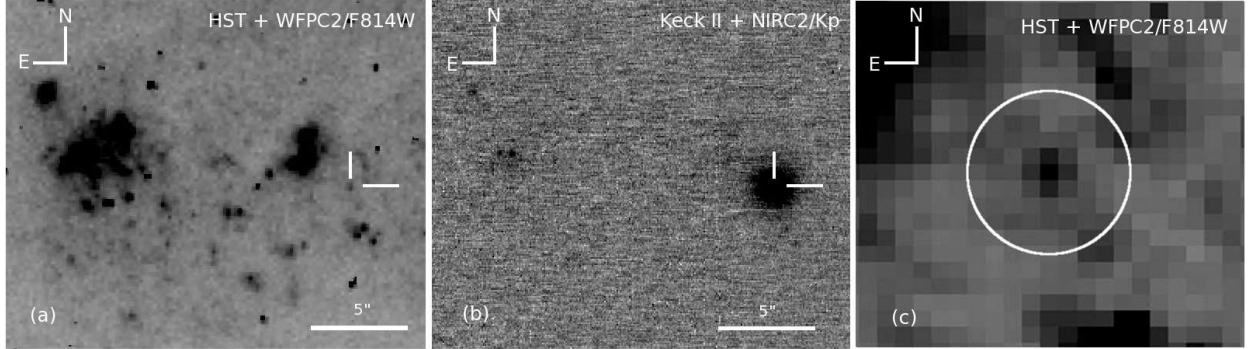


Fig. 2.— (a) Subsections of the pre-explosion *HST*+WFPC2/F814W images of NGC 1832, and (b) the post-explosion AO K_p image of SN 2009kr with Keck II+NIRC2. The approximate positions of the candidate progenitor and the SN are indicated by tick marks. (c) $5'' \times 5''$ zoom of the *HST* image. The radius circle is 3σ .

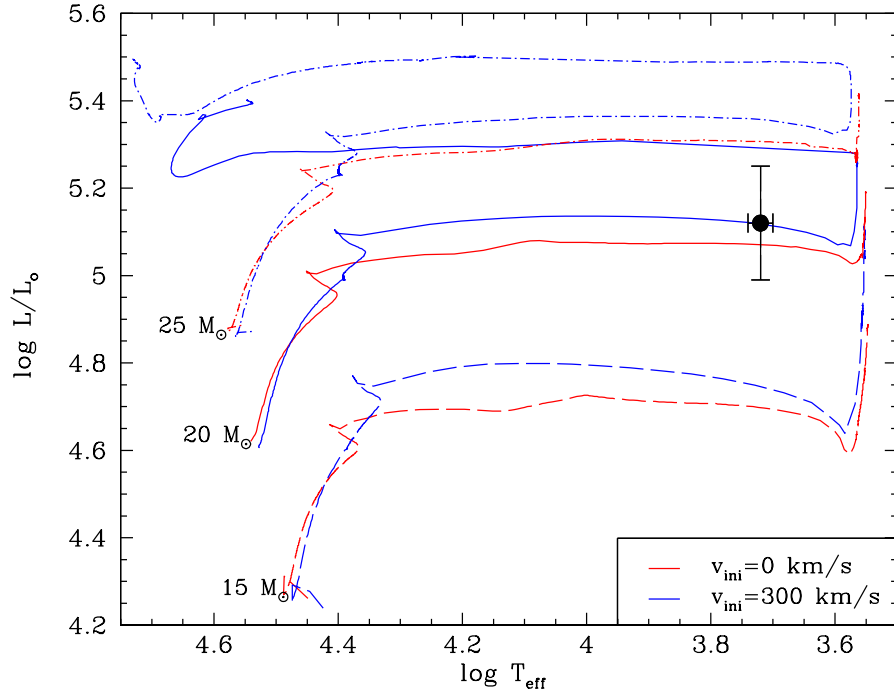


Fig. 3.— A Hertzsprung-Russell diagram showing the L_{bol} and T_{eff} for the candidate progenitor of SN 2009kr (*filled circle*). Model stellar evolutionary tracks for solar metallicity (Hirschi, Meynet, & Maeder 2004) are also shown for a rotation of $v_{\text{ini}} = 0$ km s $^{-1}$ (*dot-dashed, solid and dashed red lines*) and $v_{\text{ini}} = 300$ km s $^{-1}$ (*dot-dashed, solid and dashed blue lines*).

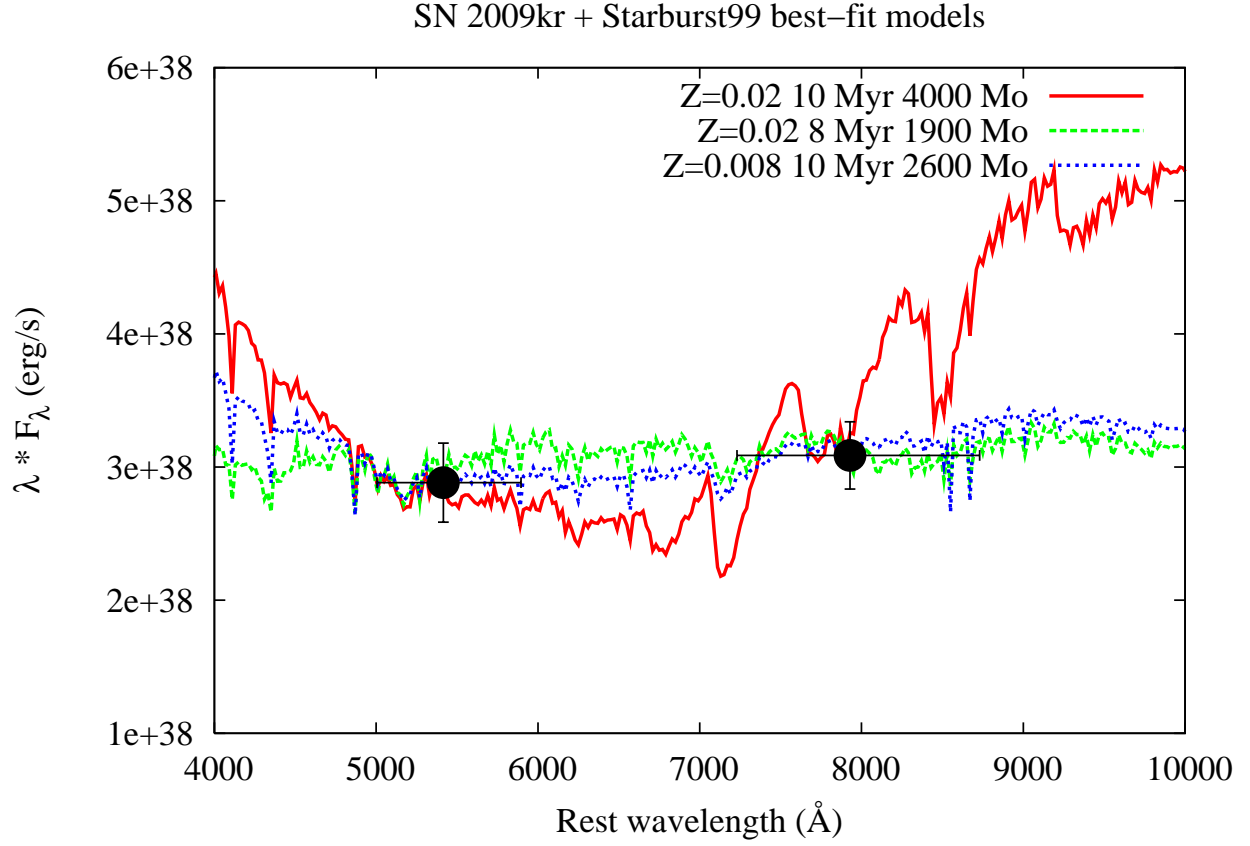


Fig. 4.— Model spectral energy distributions for star clusters (Vazquez & Leitherer 2005; *lines*) and SN 2009kr observations (*filled circles*). The model parameters (metallicity, age, total mass) are indicated in the figure.

Table 1. SN and Progenitor Candidate Position Comparison

| | $V (\alpha/\delta)$ | $I (\alpha/\delta)$ |
|--|---------------------|---------------------|
| Uncertainty in the progenitor position (mas) | 0/2 | 0/24 |
| Uncertainty in the SN position (mas) | 8/13 | 8/13 |
| Geometric transformation (mas) | 4/15 | 5/13 |
| Total uncertainty (mas) | 9/20 | 9/30 |
| Difference in position (mas) | 13/4 | 7/22 |

Note. — Uncertainties in the SN and candidate position, in milliarcsec (mas), were estimated as the standard deviation of the average. Geometric transformation errors are derived from the positional differences between the fiducial stars used in the transformation. The total uncertainty is the quadrature sum of these uncertainties. The last line lists the residual difference between the SN and progenitor position after the geometric transformation.